

Notes on the function **gsw_CT_from_rho(rho,SA,p)**

Notes written 16th April 2011

This function, **gsw_CT_from_rho(rho,SA,p)**, calculates the Conservative Temperature Θ corresponding to the input values of *in situ* density, rho, Absolute Salinity, SA, and pressure, p. The function returns NaNs if

- (i) the input density is too small (which would require Θ to exceed 40 °C), if
- (ii) the input density exceeds the density at the temperature of maximum density (as given by **gsw_CT_maxdensity(SA,p)**), or if
- (ii) the temperature is less than the freezing temperature as given by **gsw_CT_freezing(SA,p)** (implying that we are assuming that at the freezing temperature, the seawater is saturated with air).

This function, **gsw_CT_from_rho(rho,SA,p)**, uses the 48-term rational function expression for density $\rho = \hat{\rho}^{48}(S_A, \Theta, p)$ as described in appendix A.30 and appendix K of the TEOS-10 Manual (IOC *et al.* (2010)).

This function begins by calculating the freezing temperature, CT_freezing, and the thermal expansion coefficient, **gsw_alpha(SA,CT_freezing,p)** at this temperature. If this thermal expansion coefficient is positive and exceeds $1 \times 10^{-5} \text{ K}^{-1}$, a modified Newton-Raphson iterative solution procedure is performed with an initial Θ value given by solving a quadratic in Θ , given the thermal expansion coefficient at the freezing temperature and the value of density at $\Theta = 40^\circ\text{C}$, as given by **gsw_rho(SA,40,p)**. This quadratic is based on a Taylor series expression for density, expanded about the freezing temperature.

If the thermal expansion coefficient at the freezing temperature is less than $1 \times 10^{-5} \text{ K}^{-1}$ (which occurs only for Absolute Salinities less than approximately 28 g kg^{-1} , depending on pressure), the temperature of maximum density is found from **gsw_CT_maxdensity(SA,p)**. Again a simple quadratic for Conservative Temperature is solved using the density at this value of Θ and the density at $\Theta = 40^\circ\text{C}$. This quadratic gives two solutions, and if the larger of the two solutions exceeds **gsw_CT_maxdensity(SA,p)** by more than 5°C there will be only one non-frozen solution and we find this solution by the modified Newton-Raphson technique.

If the larger of these two quadratic solutions exceeds **gsw_CT_maxdensity(SA,p)** by less than 5°C we avoid using the modified Newton-Raphson method and instead solve for temperature assuming that the variation of density with Θ is a quadratic function of Θ about the temperature of maximum density. This is done iteratively, with each iteration using the previous iteration to effectively estimate $\rho_{\Theta\Theta}$ at the temperature of maximum density. In this part of the code, care is taken to distinguish cases where there are two valid solutions, both of which exceed the freezing temperature, from the situation where this is only one such solution.

When the modified Newton-Raphson method is used, three iterations are performed after which the density of the solution equals that of the input density to machine precision ($1.6 \times 10^{-12} \text{ kg m}^{-3}$). When the iterative quadratic method is used, seven iterations are performed after which the density of each non-frozen solution equals that of the input density to machine precision ($4.6 \times 10^{-13} \text{ kg m}^{-3}$).

This function **gsw_CT_from_rho**(rho,SA,p) is called as

```
[CT,CT_multiple] = gsw_CT_from_rho(rho,SA,p)
```

and if there is a valid second solution, it is returned as CT_multiple. When there is only one solution, CT_multiple is a Nan. When there are no solutions, both CT and CT_multiple are Nans.

References

IOC, SCOR and IAPSO, 2010: *The international thermodynamic equation of seawater – 2010: Calculation and use of thermodynamic properties*. Intergovernmental Oceanographic Commission, Manuals and Guides No. 56, UNESCO (English), 196 pp. Available from <http://www.TEOS-10.org>

Here follows appendix A.30 and appendix K of the TEOS-10 Manual (IOC *et al.* (2010)).

A.30 Computationally efficient 48-term expression for the density of seawater in terms of Θ

Ocean models to date have treated their salinity and temperature variables as being Practical Salinity S_p and potential temperature θ . Ocean models that are TEOS-10 compatible need to carry Preformed Salinity S_* and Conservative Temperature Θ as their conservative prognostic variables (as discussed in appendices A.20 and A.21), and they need a computationally efficient expression for density in terms of Absolute Salinity S_A , Conservative Temperature Θ and pressure p .

Following the work of McDougall *et al.* (2003) and Jackett *et al.* (2006), the TEOS-10 density ρ has been approximated by a 48-term rational. The fitted expression is the ratio of two polynomials of (S_A, Θ, p)

$$\rho \approx \rho^{48} = P_{\text{num}}^{\rho 48} / P_{\text{denom}}^{\rho 48} . \quad (\text{A.30.1})$$

The density data has been fitted in a “funnel” of data points in (S_A, Θ, p) space (McDougall *et al.* (2013)). The “funnel” extends to a pressure of 8000 dbar. At the sea surface the “funnel” covers the full range of temperature and salinity while for pressures greater than 6500 dbar, the maximum temperature of the fitted data is 10°C and the minimum Absolute Salinity is 30 g kg⁻¹. That is, the fit has been performed over a region of parameter space which includes water that is approximately 8°C warmer and 5 g kg⁻¹ fresher in the deep ocean than the seawater which exists in the present ocean. Table K.1 of appendix K contains the 48 coefficients of the expression (A.30.1) for density in terms of (S_A, Θ, p) .

As outlined in appendix K, this 48-term rational-function expression for ρ yields the thermal expansion and saline contraction coefficients, α^Θ and β^Θ , that are essentially as accurate as those derived from the full TEOS-10 Gibbs function for data in the “oceanographic funnel”. The sound speed derived by differentiating Eqn. (A.30.1) with respect to pressure has an r.m.s. error in the “funnel” of 0.067 m s⁻¹ whereas TEOS-10 fits

the available sound speed data with an rms error of only 0.035 m s^{-1} (Table O.1 of appendix O), so the sound speed obtained from the 48-term expression for density is not quite as accurate as from the full TEOS-10 expression.

In dynamical oceanography it is the thermal expansion and haline contraction coefficients α^Θ and β^Θ which are the most important aspects of the equation of state since the “thermal wind” is proportional to $\alpha^\Theta \nabla_p \Theta - \beta^\Theta \nabla_p S_A$ and the vertical static stability is given in terms of the buoyancy frequency N by $g^{-1} N^2 = \alpha^\Theta \Theta_z - \beta^\Theta (S_A)_z$. Hence for dynamical oceanography we may take the 48-term rational function expression for density, Eqn. (A.30.1), as essentially reflecting the full accuracy of TEOS-10. This is confirmed in Fig. A.30.1 where the error in using the 48-term expression for density to calculate the isobaric northward density gradient is shown. The vertical axis on this figure is the magnitude of the difference in the northward isobaric density gradient in the world ocean below 1000m when evaluated using Eqn. (A.30.1) versus using the full TEOS-10 Gibbs function. The scales of the axes of this figure have been chosen to be the same as those of Fig. A.5.1 of appendix A.5 so that the smallness of the errors incurred by using the 48-term density expression can be appreciated. By comparing Figs. A.30.1 and A.5.1 it is clear that the much more important issue is to properly represent the effects of seawater composition on seawater density, and this aspect of ocean science is in its infancy. The rms value of the vertical axis in Fig. A.30.1 is 4.6% of that of Fig. A.5.1.

Appendix P describes how an expression for the enthalpy of seawater in terms of Conservative Temperature, specifically the functional form $\hat{h}(S_A, \Theta, p)$, together with an expression for entropy in the form $\hat{\eta}(S_A, \Theta)$, can be used as an alternative thermodynamic potential to the Gibbs function $g(S_A, t, p)$. The need for the functional form $\hat{h}(S_A, \Theta, p)$ also arises in section 3.32 and in Eqns. (3.26.3) and (3.29.1). The 48-term expression, Eqn. (A.30.1), for $\rho^{48} = \hat{\rho}^{48}(S_A, \Theta, p)$ can be used to find a closed expression for $\hat{h}(S_A, \Theta, p)$ by integrating the reciprocal of $\hat{\rho}^{48}(S_A, \Theta, p)$ with respect to pressure (in Pa), since $\hat{h}_p = v = \rho^{-1}$ (see Eqn. (2.8.3)).

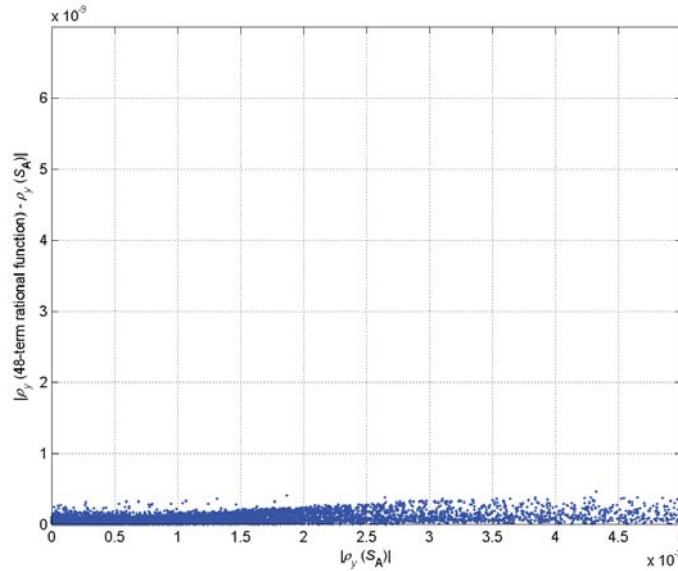


Figure A.30.1. The northward density gradient at constant pressure (the horizontal axis) for data in the world ocean atlas of Gouretski and Koltermann (2004) for $p > 1000$ dbar. The vertical axis is the magnitude of the difference between evaluating the density gradient using the 48-term expression Eqn. (A.30.1) instead of using the full TEOS-10 expression, using Absolute Salinity S_A as the salinity argument in both cases.

The 48-term expression for specific volume, Eqn. (A.30.1), is first written explicitly as the ratio of two polynomials in sea pressure p (in dbar) as

$$\hat{v}^{48} = \frac{1}{\hat{\rho}^{48}} = \frac{a_0 + a_1 p + a_2 p^2 + a_3 p^3}{b_0 + 2b_1 p + b_2 p^2}, \quad (\text{A.30.2})$$

where the coefficients a_0 to a_3 and b_0 to b_2 are the following functions of S_A and Θ

$$\begin{aligned} a_0 &= v_{21} + v_{22}\Theta + v_{23}\Theta^2 + v_{24}\Theta^3 + v_{25}\Theta^4 + S_A (v_{26} + v_{27}\Theta + v_{28}\Theta^2 + v_{29}\Theta^3 + v_{30}\Theta^4) \\ &\quad + (S_A)^{1.5} (v_{31} + v_{32}\Theta + v_{33}\Theta^2 + v_{34}\Theta^3 + v_{35}\Theta^4) + v_{36}S_A^2, \\ a_1 &= v_{37} + v_{38}\Theta + v_{39}\Theta^2 + v_{40}\Theta^3 + S_A (v_{41} + v_{42}\Theta), \\ a_2 &= v_{43} + v_{44}\Theta + v_{45}\Theta^2 + v_{46}\Theta S_A, \\ a_3 &= v_{47} + v_{48}\Theta, \\ b_0 &= v_{01} + v_{02}\Theta + v_{03}\Theta^2 + v_{04}\Theta^3 + S_A (v_{05} + v_{06}\Theta + v_{07}\Theta^2) + (S_A)^{1.5} (v_{08} + v_{09}\Theta + v_{10}\Theta^2 + v_{11}\Theta^3), \\ b_1 &= 0.5(v_{12} + v_{13}\Theta + v_{14}\Theta^2 + S_A (v_{15} + v_{16}\Theta)), \\ b_2 &= v_{17} + v_{18}\Theta + v_{19}\Theta^2 + v_{20}S_A, \end{aligned}$$

and the numbered coefficients v_1 to v_{48} can be found in Table K.1 (note that $v_{21} = 1$).

It is not difficult to rearrange Eqn. (A.30.2) into the form

$$\hat{v}^{48} = \hat{v}^{48}(S_A, \Theta, p) = \left(\frac{a_2}{b_2} - \frac{2a_3b_1}{b_2^2} \right) + \frac{a_3}{b_2} p + \frac{N + Mp}{b_0 + 2b_1 p + b_2 p^2}, \quad (\text{A.30.3})$$

where N and M are given by

$$N = a_0 + \frac{2a_3b_0b_1}{b_2^2} - \frac{a_2b_0}{b_2}, \quad \text{and} \quad M = a_1 + \frac{4a_3b_1^2}{b_2^2} - \frac{a_3b_0}{b_2} - \frac{2a_2b_1}{b_2}. \quad (\text{A.30.4})$$

The pressure integral of the last term in Eqn. (A.30.3) is well known (see for example section 2.103 of Gradshteyn and Ryzhik (1980)) and is dependent on the sign of the discriminant of the denominator. In our case it can be shown that $b_1^2 > b_0b_2$ over the full TEOS-10 (S_A, Θ, p) domain, and also that b_0 is positive while both b_1 and b_2 are negative and bounded away from zero over the full TEOS-10 (S_A, Θ, p) domain. The indefinite integral, with respect to pressure measured in Pa, of the last term in Eqn. (A.30.3) is (with $N^* = 10^4 N$ and $M^* = 10^4 M$)

$$\int \frac{N + Mp}{b_0 + 2b_1 p + b_2 p^2} dP' = \frac{M^*}{2b_2} \ln |b_0 + 2b_1 p + b_2 p^2| + \frac{N^*b_2 - M^*b_1}{2b_2\sqrt{b_1^2 - b_0b_2}} \ln \left| \frac{b_2 p + b_1 - \sqrt{b_1^2 - b_0b_2}}{b_2 p + b_1 + \sqrt{b_1^2 - b_0b_2}} \right|, \quad (\text{A.30.5})$$

The enthalpy $\hat{h}^{48}(S_A, \Theta, p)$ is the definite integral of Eqn. (A.30.3) from P_0 to P , plus $c_p^0 \Theta$, being the value of enthalpy at P_0 (i. e. at $p = 0$ dbar). Hence the full expression for $\hat{h}^{48}(S_A, \Theta, p)$ is (with $A = b_1 - \sqrt{b_1^2 - b_0b_2}$ and $B = b_1 + \sqrt{b_1^2 - b_0b_2}$)

$$\begin{aligned} \hat{h}^{48}(S_A, \Theta, p) &= c_p^0 \Theta + 10^4 \left(\frac{a_2}{b_2} - \frac{2a_3b_1}{b_2^2} \right) p + 10^4 \frac{a_3}{2b_2} p^2 \\ &\quad + \frac{M^*}{2b_2} \ln \left(1 + \frac{2b_1}{b_0} p + \frac{b_2}{b_0} p^2 \right) + \frac{N^* - \frac{b_1}{b_2} M^*}{(B-A)} \ln \left(1 + p \frac{b_2}{A} \frac{(B-A)}{(B+b_2 p)} \right). \end{aligned} \quad (\text{A.30.6})$$

The factor of 10^4 that appears here and in N^* and M^* effectively serves to convert the units of the integration variable from dbar to Pa so that $\hat{h}^{48}(S_A, \Theta, p)$ has units of J kg^{-1} . In these equations S_A is in g kg^{-1} , Θ in $^\circ\text{C}$ and p is in dbar. The arguments of the two natural logarithms in Eqn. (A.30.6) are always positive; over the full TEOS-10 (S_A, Θ, p)

domain the argument of the first logarithm term is between 0.4 and 1.0 while the argument of the second logarithm term is between 1.0 and 3.5 (note that both b_2 and A are negative while B is positive). Specific enthalpy calculated from Eqn. (A.30.6) is available in the GSW Oceanographic Toolbox as the function **gsw_enthalpy**(SA,CT,p). The evaluation of $\hat{h}^{48}(S_A, \Theta, p)$ via Eqn. (A.30.6) takes just 12% more computer cpu time than the evaluation of $\hat{v}^{48}(S_A, \Theta, p)$ via a computationally efficient (Hornered in terms of Θ, S_A and p) version of Eqn. (A.30.1). The use of Eqn. (A.30.6) and **gsw_enthalpy** to evaluate $\hat{h}^{48}(S_A, \Theta, p)$ is 9 times faster than first evaluating the in situ temperature t (from **gsw_t_from_CT**(SA,CT,p)) and then calculating enthalpy from the full Gibbs function expression $h(S_A, t, p)$ using **gsw_enthalpy_t_exact**(SA,t,p). (These last two function calls have also been combined into the one function, **gsw_enthalpy_CT_exact**(SA,CT,p).)

Also, when the enthalpy difference at the same values of S_A and Θ but at different pressures (see Eqn. (3.32.5)) is evaluated using Eqn. (A.30.6), the expression can also be arranged to contain only two logarithm terms (McDougall *et al.* (2013)). This enthalpy difference is available as the function **gsw_enthalpy_diff**(SA,CT,p) in the GSW Toolbox.

Following Young (2010), the difference between h and $c_p^0 \Theta$ is called “dynamic enthalpy” and can be calculated from Eqn. (A.30.6). Dynamic enthalpy is available in the GSW Oceanographic Toolbox as the function **gsw_dynamic_enthalpy**(SA,CT,p).

Appendix K: Coefficients of 48-term expression for the density of seawater in terms of Θ

The TEOS-10 Gibbs function of seawater $g(S_A, t, p)$ is written as a polynomial in terms of in situ temperature t , while for ocean models, density needs to be expressed as a computationally efficient expression in terms of Conservative Temperature Θ . McDougall *et al.* (2013) have fitted the TEOS-10 values of density ρ to S_A , Θ and p in a “funnel” of data points in (S_A, Θ, p) space. The fitted expression is in the form of a rational function, being the ratio of two polynomials of (S_A, Θ, p)

$$\rho = P_{\text{num}}^{\rho 48} / P_{\text{denom}}^{\rho 48}. \quad (\text{K.1})$$

The “funnel” of data points in (S_A, Θ, p) space is shown in Figure K.1 and is described in more detail in McDougall *et al.* (2013); at the sea surface it covers the full range of temperature and salinity while for pressure greater than 6500 dbar, the maximum temperature of the fitted data is 10°C and the minimum Absolute Salinity is 30 g kg⁻¹. The maximum pressure of the “funnel” is 8000 dbar. Table K.1 contains the 48 coefficients of the expression (K.1) for density in terms of (S_A, Θ, p) . The coefficients v_1-v_{20} in this table have units of kg m⁻³ and the coefficients $v_{21}-v_{48}$ are dimensionless, and the normalizing values of S_A , Θ and p are 1 g kg⁻¹, 1 K and 1 dbar respectively.

The rms error of this 48-term approximation to the TEOS-10 density over the “funnel” is 0.00046 kg m⁻³; this can be compared with the rms uncertainty of 0.004 kg m⁻³ of the underlying laboratory density data to which the TEOS-10 Gibbs function was fitted (see the first two rows of Table O.1 of appendix O). Similarly, the appropriate thermal expansion coefficient,

$$\alpha^\Theta = - \frac{1}{\rho} \left. \frac{\partial \rho}{\partial \Theta} \right|_{S_A, p}, \quad (\text{K.2})$$

of the 48-term equation of state is different from the same thermal expansion coefficient evaluated from TEOS-10 with an rms error in the “funnel” of $0.069 \times 10^{-6} \text{ K}^{-1}$, compared with the rms error of the thermal expansion coefficient of the laboratory data to which the Feistel (2008) Gibbs function was fitted of $0.73 \times 10^{-6} \text{ K}^{-1}$ (see row six of Table O.1 of appendix O). In terms of the evaluation of density gradients, the haline contraction coefficient evaluated from Eqn. (K.1) is many times more accurate than the thermal expansion coefficient. Hence we may consider the 48-term rational function expression for density, Eqn. (K.1), to be equally as accurate as the full TEOS-10 expressions for density, for the thermal expansion coefficient and for the haline contraction coefficient for data that reside inside the “oceanographic funnel”.

The sound speed evaluated from the 48-term rational function Eqn. (K.1), has an rms error over the “funnel” of 0.067 m s^{-1} which is almost twice the r.m.s. error of the underlying sound speed data that was incorporated into the Feistel (2008) Gibbs function, being 0.035 m s^{-1} (see rows 7 to 9 of Table O.1 of appendix O). Hence, the 48-term expression for density is not quite as accurate as the full TEOS-10 for evaluating sound speed in the ocean. But for dynamical oceanography where α^Θ and β^Θ are the aspects of the equation of state that, together with spatial gradients of S_A and Θ , drive ocean currents and affect the calculation of the buoyancy frequency, we may take the 48-term rational-function expression for density, Eqn. (K.1), as essentially reflecting the full

accuracy of TEOS-10. The accuracy of the 48-term rational function expression for density is illustrated as a function of pressure in Fig. K.2.

The use of Eqn. (K.1) to evaluate $\hat{\rho}^{48}(S_A, \Theta, p)$ from **gsw_rho_CT**(S_A, CT, p) is 6.4 times faster than first evaluating the in situ temperature t (from **gsw_t_from_CT**(S_A, CT, p)) and then calculating in situ density from the full Gibbs function expression $\rho(S_A, t, p)$ via **gsw_rho_t_exact**(S_A, t, p). (These last two function calls have been combined into **gsw_rho_CT_exact**(S_A, CT, P).)

	P_{num}^{48}	Coefficients (kg m^{-3})		P_{denom}^{48}	Coefficients (unitless)
v_{01}		$9.998\,420\,897\,506\,056 \times 10^2$	v_{21}		1.0
v_{02}	Θ	$2.839\,940\,833\,161\,907 \times 10^0$	v_{22}	Θ	$2.775\,927\,747\,785\,646 \times 10^{-3}$
v_{03}	Θ^2	$-3.147\,759\,265\,588\,511 \times 10^{-2}$	v_{23}	Θ^2	$-2.349\,607\,444\,135\,925 \times 10^{-5}$
v_{04}	Θ^3	$1.181\,805\,545\,074\,306 \times 10^{-3}$	v_{24}	Θ^3	$1.119\,513\,357\,486\,743 \times 10^{-6}$
v_{05}	S_A	$-6.698\,001\,071\,123\,802 \times 10^0$	v_{25}	Θ^4	$6.743\,689\,325\,042\,773 \times 10^{-10}$
v_{06}	$S_A \Theta$	$-2.986\,498\,947\,203\,215 \times 10^{-2}$	v_{26}	S_A	$-7.521\,448\,093\,615\,448 \times 10^{-3}$
v_{07}	$S_A \Theta^2$	$2.327\,859\,407\,479\,162 \times 10^{-4}$	v_{27}	$S_A \Theta$	$-2.764\,306\,979\,894\,411 \times 10^{-5}$
v_{08}	$(S_A)^{1.5}$	$-3.988\,822\,378\,968\,490 \times 10^{-2}$	v_{28}	$S_A \Theta^2$	$1.262\,937\,315\,098\,546 \times 10^{-7}$
v_{09}	$(S_A)^{1.5} \Theta$	$5.095\,422\,573\,880\,500 \times 10^{-4}$	v_{29}	$S_A \Theta^3$	$9.527\,875\,081\,696\,435 \times 10^{-10}$
v_{10}	$(S_A)^{1.5} \Theta^2$	$-1.426\,984\,671\,633\,621 \times 10^{-5}$	v_{30}	$S_A \Theta^4$	$-1.811\,147\,201\,949\,891 \times 10^{-11}$
v_{11}	$(S_A)^{1.5} \Theta^3$	$1.645\,039\,373\,682\,922 \times 10^{-7}$	v_{31}	$(S_A)^{1.5}$	$-3.303\,308\,871\,386\,421 \times 10^{-5}$
v_{12}	p	$-2.233\,269\,627\,352\,527 \times 10^{-2}$	v_{32}	$(S_A)^{1.5} \Theta$	$3.801\,564\,588\,876\,298 \times 10^{-7}$
v_{13}	$p \Theta$	$-3.436\,090\,079\,851\,880 \times 10^{-4}$	v_{33}	$(S_A)^{1.5} \Theta^2$	$-7.672\,876\,869\,259\,043 \times 10^{-9}$
v_{14}	$p \Theta^2$	$3.726\,050\,720\,345\,733 \times 10^{-6}$	v_{34}	$(S_A)^{1.5} \Theta^3$	$-4.634\,182\,341\,116\,144 \times 10^{-11}$
v_{15}	$p S_A$	$-1.806\,789\,763\,745\,328 \times 10^{-4}$	v_{35}	$(S_A)^{1.5} \Theta^4$	$2.681\,097\,235\,569\,143 \times 10^{-12}$
v_{16}	$p \Theta S_A$	$6.876\,837\,219\,536\,232 \times 10^{-7}$	v_{36}	S_A^2	$5.419\,326\,551\,148\,740 \times 10^{-6}$
v_{17}	p^2	$-3.087\,032\,500\,374\,211 \times 10^{-7}$	v_{37}	p	$-2.742\,185\,394\,906\,099 \times 10^{-5}$
v_{18}	$p^2 \Theta$	$-1.988\,366\,587\,925\,593 \times 10^{-8}$	v_{38}	$p \Theta$	$-3.212\,746\,477\,974\,189 \times 10^{-7}$
v_{19}	$p^2 \Theta^2$	$-1.061\,519\,070\,296\,458 \times 10^{-11}$	v_{39}	$p \Theta^2$	$3.191\,413\,910\,561\,627 \times 10^{-9}$
v_{20}	$p^2 S_A$	$1.550\,932\,729\,220\,080 \times 10^{-10}$	v_{40}	$p \Theta^3$	$-1.931\,012\,931\,541\,776 \times 10^{-12}$
			v_{41}	$p S_A$	$-1.105\,097\,577\,149\,576 \times 10^{-7}$
			v_{42}	$p \Theta S_A$	$6.211\,426\,728\,363\,857 \times 10^{-10}$
			v_{43}	p^2	$-1.119\,011\,592\,875\,110 \times 10^{-10}$
			v_{44}	$p^2 \Theta$	$-1.941\,660\,213\,148\,725 \times 10^{-11}$
			v_{45}	$p^2 \Theta^2$	$-1.864\,826\,425\,365\,600 \times 10^{-14}$
			v_{46}	$p^2 \Theta S_A$	$1.119\,522\,344\,879\,478 \times 10^{-14}$
			v_{47}	p^3	$-1.200\,507\,748\,551\,599 \times 10^{-15}$
			v_{48}	$p^3 \Theta$	$6.057\,902\,487\,546\,866 \times 10^{-17}$

TABLE K.1 Coefficients of the polynomials $P_{\text{num}}^{48}(S_A, \Theta, p)$ and $P_{\text{denom}}^{48}(S_A, \Theta, p)$ that define the 48-term rational-function Eqn. (K.1) for density.

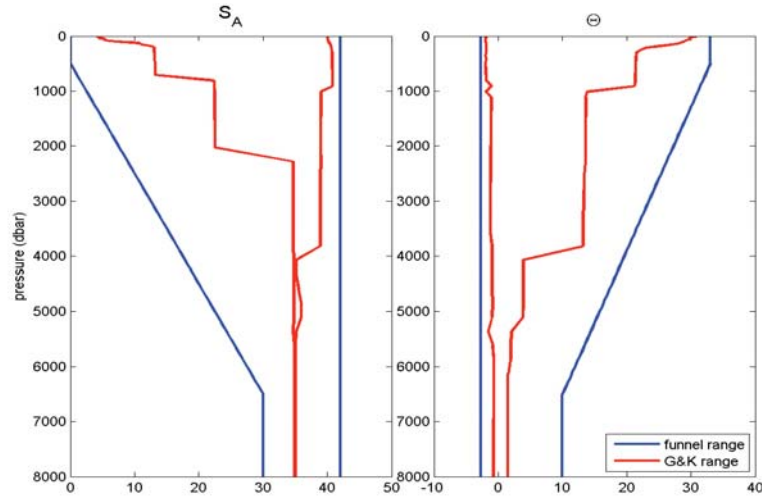


Figure K.1. The ranges of Absolute Salinity and Conservative Temperature in the “Oceanographic funnel” (the blue lines) in which the 48-term expression for density was fitted. The red lines shows the minimum and maximum values of Absolute Salinity and Conservative Temperature that occur in a hydrographic ocean atlas of the world ocean (Gouretski and Koltermann (2004)).

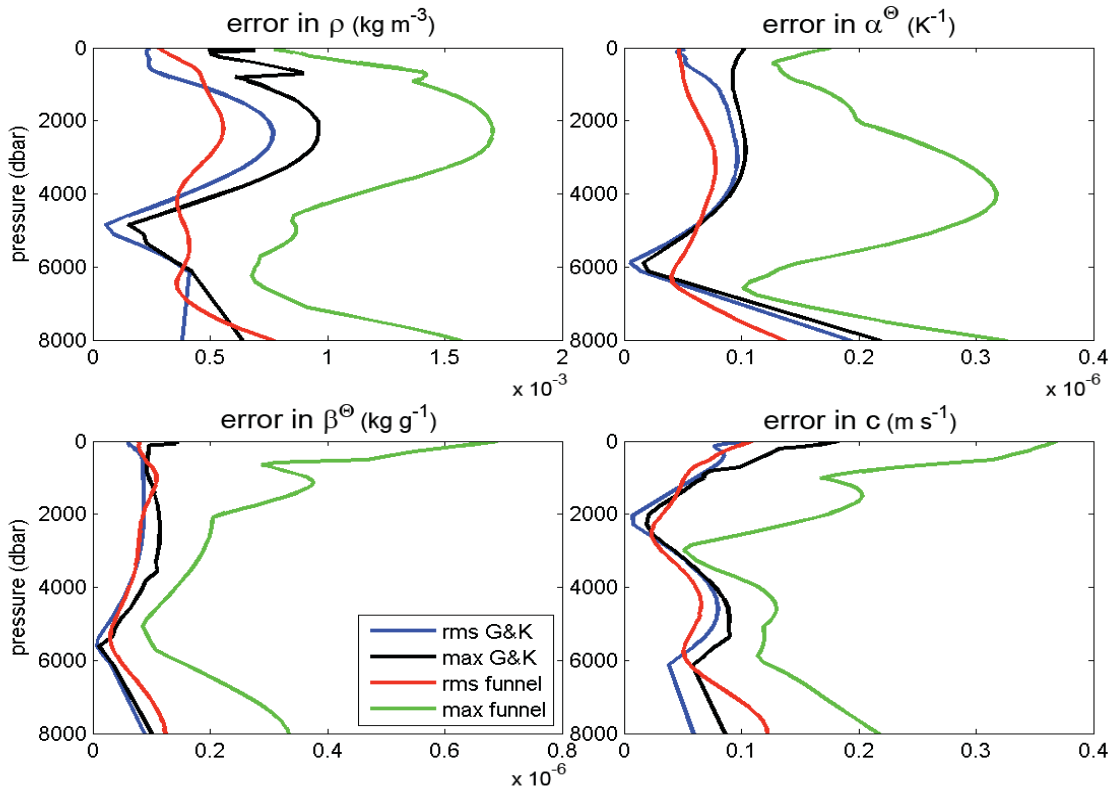


Figure K.2. The errors in using the 48-term rational function expression for density, Eqn. (K.1), to evaluate density, the thermal expansion coefficient, the saline contraction coefficient and sound speed. The red and green lines are the r.m.s. and maximum errors for seawater in the “oceanographic funnel” of McDougall *et al.* (2013), while the blue and black lines are the r.m.s. and maximum errors for data in the world ocean atlas of Gouretski and Koltermann (2004).